

# Instability on condensate propagation in porous media

Eko Siswanto, Hiroshi Katsurayama, and Yasuo Katoh

**Abstract**—Instability on condensate propagation in porous bed of glass-beads and alumina-balls media is observed experimentally. This study is done by streaming the varied temperature of saturated humid-air over the media. Towards the humid air temperatures, the ambient temperatures are restrained on constant 308 K and on constant-ratio, respectively. By calculated evaluation, it is clear that the condensate propagation is in Darcian regime. In this theoretically stable regime, however, based on visualization and on modified Lyapunov-exponent for the longest finger, the propagation lies respectively on stable-dominant, unstable-dominant, and temporal-chaos behavior. It is known that the instability propagation is not only depended on porosity and permeability, but also controlled by wettability of the porous media and concentration gradient of the condensate in the porous layer. From this study, it is also evident that the ambient temperature plays a key role on generating the concentration gradient.

**Keywords**—Instability propagation, Lyapunov exponent, Glass beads, Alumina balls, Wettability.

## I. INTRODUCTION

CAPILLARY pumping on multiphase system has been implemented widely for electronic cooling, satellite thermal control, and other space application due to it does not need of any mechanical pump for driving the fluid [1]. Regarding to capability on capillary pumping in the vacuum as well, i.e., forced by wetting process, porous media becomes an important alternative device to the space duties. In this current paper, study on the porous media is intended for controlling humidity.

Ability in both extracting and releasing moist from/to air is fundamental performance of porous media in the controlling humidity purpose. Because of the moist extraction or condensation is one of crucial stages in that purpose, therefore, condensate migration in the media becomes important due to have direct relation with the extraction rate.

Manuscript received July 30, 2011.

E.S. is with the Yamaguchi University, Science and Engineering, Mechanical Engineering Dept., 2-16-1 Tokiwadai, Ube, Yamaguchi 755-8611, Japan (phone: +8180-3873-2678; fax: +81836-85-9101; e-mail: m505wc@yamaguchi-u.ac.jp), on leave from Brawijaya University, Mechanical Eng. Dept., Malang, Indonesia (e-mail: eko\_s112@ub.ac.id).

H.K. is with the Yamaguchi University, Science and Engineering, Mechanical Engineering Dept., 2-16-1 Tokiwadai, Ube, Yamaguchi 755-8611, Japan (e-mail: katsura@yamaguchi-u.ac.jp).

Y.K. is with the Yamaguchi University, Science and Engineering, Mechanical Engineering Dept., 2-16-1 Tokiwadai, Ube, Yamaguchi 755-8611, Japan (e-mail: ykatoh@yamaguchi-u.ac.jp).

TABLE I  
SYMBOL, QUANTITY, AND UNIT

Symbol	Quantity	Unit
$C_{p1}, C_{ph}$	heat capacity of <i>condensate, mixture</i>	J/kg·K
$d$	diameter of particle	m
$D_0, D_n, D_{n+1}$	(numerical) distance on <i>initial, n, n+1</i> iteration	-
$g$	acceleration of gravity	kg·m/s <sup>2</sup>
$Gr$	Grashof number	-
$h_{av}$	average ascend-height of water	m
$h_{fg}$	latent heat of condensation	J/kg
$Ja$	Jacob number	-
$K$	Rumpf-Gupte permeability	m <sup>2</sup>
$Ku$	Kutaleladze number	-
$l$	characteristic length	m
$L$	Lyapunov Exponent ( <i>LE</i> )	-
$N$	number of total iteration or cycles	-
$Pr$	Prandtl number	-
$r_{eq}$	porous channel radius equivalent	m
$R_{av}$	average $R_n$	-
$R_n$	instantaneous <i>LE</i> series	-
$S_n, S_{n+1}$	(observed) distance on <i>n, n+1</i> cycles	m
$T_a, T_h$	temperatures of <i>ambient, mixture</i>	K
$T_c$	temperature of cooper plate	K
$T_f, T_b, T_t$	temperature of <i>front, back, top</i> of wall = $\sim T_a$	K
$T_s$	interface temperature	K
$T_w$	average temperature of chamber-walls = $[T_c + (T_f + T_b + T_t)]/4$	K
$W_a, W_i, W_s$	work of <i>adhesion, immersion, spreading</i>	N/m
$\Delta T$	temperature difference = $T_h - T_w$	K
$\varepsilon$	porosity of porous bed	-
$\theta$	wetting angle of porous bed	°
$\xi$	perturbation parameter	-
$\rho, \rho_l, \rho_v, \rho_p$	density of <i>water, condensate, vapor, particle</i>	kg/m <sup>3</sup>
$\sigma$	surface tension of water	N/m
$\chi^2$	porous bed shape parameter = $\varepsilon l^2 / K$	-

Basically, based on simple balance between capillary and viscous force, wetting phenomena between fluid and porous media was unpredictable [2]. It means, experimentally, fluid migration and/or propagation in the porous media takes place with complex flow. In contrast, most of analytical studies of condensate in porous media were simplified at 2-D and uniform-flow [3]-[7].

Hence, although the studies have already taken into account permeability [3]-[5], surface tension [6], and gravity [7], however, those only informed uniform flow cases. For the reasons, this study is intended to explore experimentally dynamics of condensate migration conducted in a (3D)

chamber and, also considers wettability, obtained from a test, of the media. For this wettability, glass-beads and alumina-balls are used as the porous media.

Our experiences [8]-[10] identified that there were two steps of condensate flow mechanism into porous media in a plain system. Vapor condensed firstly on upper-face (interface) of media, and then the condensate migrated and/or propagated down by penetrating the media. As already discussed, the resulted condensate was depended on thermal conductivity of particles of media [8] since it influenced temperature of the interface [9], [10], while heat fluxes, which crossed the interface, affected its efficiency [10]. From the experience, it is known that the studies were still based on heat flux components, i.e., heat transfer dynamics, toward globally extracted condensate. Therefore, by treating ambient temperatures, this study is focused on local migration of the condensate, i.e., mass flow (of finger propagation) dynamics.

Respect to the dynamics, this study employs a widely-used Lyapunov-exponent (*LE*) base method, other than visualization, to classify the migration. Selection of this method is due to its calculation is able to do fast and reliable [11]. The *LE*-base method was applied to indicate growth rate of perturbation of attractor on continuous- [12], [13], and discrete-dynamics models [14], [15], and on experiment cases [16]. In [11] and [15] studies, a practical *LE* computing evolution of two attractors separation was proposed. However, there is a note on the computation, namely, substitution with a given initial constant-separation in the each iteration. Thus, if this notion is applied directly in this migration, then, after the constant separation is exceeded, the exponent is always in positive values although a leading attractor (a chosen propagation point) in stagnant toward a lagging (other chosen point) one. Due to information represents stagnant-, simultaneous-, and convergent-attractors are also crucial in this dynamics, then a modified practical *LE*, without substitution of the constant separation, is also presented in this study.

## II. EXPERIMENTAL METHOD

### A. Porous Media Properties Test

Based on the basic particle properties (see Table II), porous bed properties were tested and determined.

TABLE II  
PARTICLE PROPERTIES

Particle	$d \times 10^{-3}$	$\rho_p \times 10^3$	Composition
Glass beads	1.0	2.60	Soda glass
Alumina balls	1.0	3.61	Al <sub>2</sub> O <sub>3</sub> :94.5% SiO <sub>2</sub> :5.5%

After porosity  $\epsilon$  of the bed was calculated using a direct test, Rumpf-Gupte permeability  $K$  of spherical particles bed was then defined as [17],

$$K = \epsilon^{5.5} d^2 / 5.6 \quad (1)$$

Porous channel radius equivalent  $r_{eq}$  was calculated as,

$$r_{eq} = \epsilon d / [3(1 - \epsilon)] \quad (2)$$

By using capillary-rise test proposed in [18], average ascend-height  $h_{av}$  of liquid was measured. Wetting angle of the media bed  $\theta$  was then determined.

$$r_{eq} = 2\sigma \cos \theta / (\rho g h_{av}) \quad (3)$$

To obtain three types of wetting processes, i.e., adhesion, immersion, and spreading, the respective energy of the wettability components were calculated as [2],

$$W_a = \sigma (\cos \theta + 1) \quad (4)$$

$$W_i = \sigma \cos \theta \quad (5)$$

$$W_s = \sigma (\cos \theta - 1) \quad (6)$$

### B. Condensate Migration Test

Porous glass-beads or alumina-balls was filled in half of 0.02 m x 0.04 m x 0.24 m of condensation chamber, schematically shown in Fig. 1.

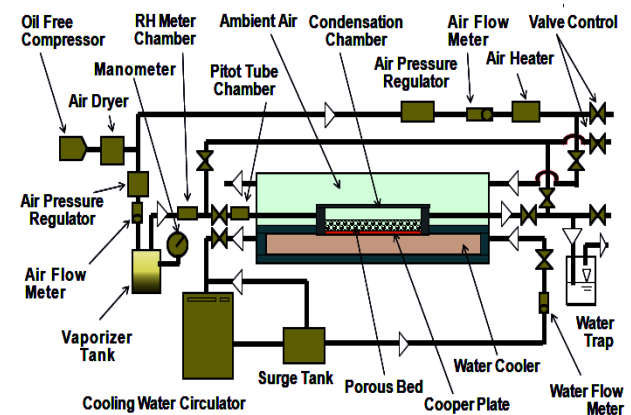


Fig.1 Schematic of experimental apparatus

Laminar of 99 %RH vapor-air mixture was streamed over the upper-face of porous media bed. Temperatures of the mixture  $T_h$  were varied at 308, 313, 318, 323, and 328 K, respectively. Ambient temperatures were controlled at  $T_a=308$  K constantly and at constant temperature-ratio  $T_h/T_a=1$ . Furthermore, to monitor the lateral condensate migration behavior, a video camera was installed for 60 minutes observation.

To assure that air supplied to all system were clean or no oil contaminant, a compressed oil-free air, through a dryer, was forced to the vapor-air and the ambient-air lines. Compressed-air supplied into vaporizer tank was maintained at  $2 \times 10^{-2}$  m<sup>3</sup>/min constantly. In ambient line, 0.175 MPa compressed-air was regulated by heater to obtain a desired temperature. Valve-controls are used to blow transient-gas out before

starting the observation, and to guarantee that the vapor- and the ambient-air settled. A water trap tank was required to reduce shock condition, i.e., pressure and temperature, of atmosphere. To maintain the copper plate temperature  $T_c$ , as bottom-face of the bed, a  $7.5 \times 10^{-4} \text{ m}^3/\text{min}$  of 283 K water was circulated by a water-cooler package attached by a surge tank.

III. RESULT AND DISCUSSION

A. Condensation on Interface and Migration Regime

A1. Condensation on interface

First of all, to evaluate whether inertia or heat transfer controls dominantly a produced condensate on the interface, as a source of migrated condensate, we uses Jacob number defined as follows [19].

$$Ja = Cp_l \rho_l \Delta T / h_{fg} \rho_v \quad (6)$$

Fig.2 contains Jacob number  $Ja$  and interface temperature  $T_s$  for both media, i.e., alumina balls (AB) and glass beads (GB), under both treatments ( $T_a=308 \text{ K}$  and  $T_h/T_a=1$ ). Jacob number for  $T_a=308 \text{ K}$  treatments are  $Ja \leq 46.99$ , whereas for  $T_h/T_a=1$  are  $Ja \leq 19.23$ . The higher  $Ja$  on the  $T_a=308 \text{ K}$  are caused by higher temperature difference  $\Delta T$  of that treatments. However, as also mentioned in the figure, all of the  $Ja$  of the both treatments are less than 100. These mean that heat transfer dominates to control condensation on the interface rather than inertia. It confirms that the ambient temperature treatments play a key role on the source of migrated condensate.

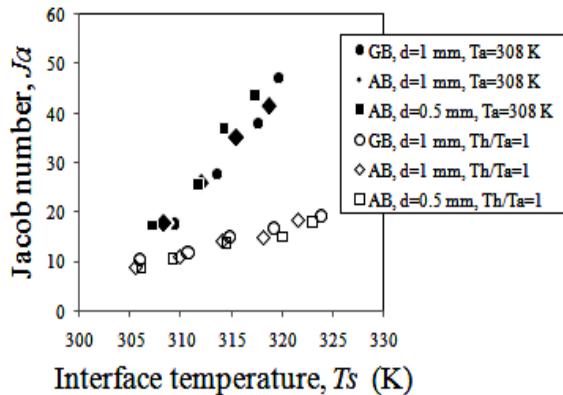


Fig.2 Interface temperature  $T_s$  and Jacob number  $Ja$

B. Migration Regime

After condensing on the interface, the condensate migrates laterally into the porous media bed. To be able to compare to a previous analytical study [20] and to locate where the migration regime lies, i.e., in Darcian or nonDarcy, it is needed to evaluate Kutaleladze number  $Ku$  or subcooling parameter, Prandtl number  $Pr$  as diffusive parameter, and perturbation parameter  $\xi$  of the system, where  $Ku$  and  $\xi$  are defined respectively as,

$$Ku = Cp_h \Delta T / h_{fg} \quad (7)$$

$$\xi = 2 \chi^2 / Gr^{0.5} \quad (8)$$

Fig.3 shows range of all of  $Ku$  values ( $2.46 \times 10^{-3} \leq Ku \leq 13.27 \times 10^{-3}$ ), and of respective  $\xi$  ( $\xi \geq 0.36 \times 10^4$  for  $d=10^{-3} \text{ m}$ , and  $\xi \geq 1.41 \times 10^4$  for  $d=0.5 \times 10^{-3} \text{ m}$ ). In this system, Prandtl number of mixture is about  $Pr = 0.7$ . Hence, by matching these results to the analytical study, this migration is then known in Darcian regime or (theoretical) uniform flow, since for the  $Pr$  and  $Ku$  range, the perturbation parameter of the system exceed the limit for non-Darcy, i.e.,  $\xi \geq 10^2$ , [20].

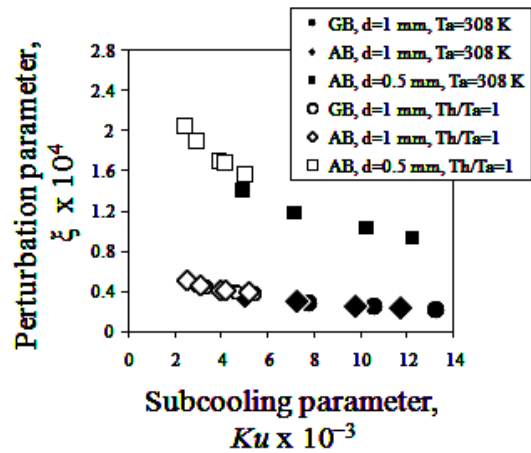


Fig.3 Subcooling- and perturbation-parameter for glass beads (GB) and alumina ball (AB)

C. Condensate Migration Dynamics

C1. Effect of wettability

Table III informs the test results for wettability components and other important porous media bed properties, under room condition (289–296 K and 47–54 %RH) for 48 hours.

TABLE III  
POROUS BED PROPERTIES

Properties	Glass beads	Alumina balls	
$d \times 10^{-3}$	1	1	0.5
$\epsilon$	0.38	0.38	0.38
$r_{eq} \times 10^{-3}$	0.204	0.204	0.102
$h_{av} \times 10^{-3}$	-2.95	2.5	33.8
$\theta$	94	87	76
$K \times 10^{-4}$	8.72	8.72	0.22
$W_a \times 10^{-3}$	64.62	70.84	84.52
$W_i \times 10^{-3}$	-3.75	2.84	16.52
$W_s \times 10^{-3}$	-71.75	-65.16	-51.48

Fig.4-7 exhibit that condensate migrates down by dynamic penetration. In the same temperature treatment (i.e., same condensate surface tension) and media (alumina balls), the condensate is detained prevalently as flat-like in upper-bed for  $d=0.5 \times 10^{-3} \text{ m}$ , as shown in Fig.4, whereas channels (vertical line) appear in  $d=10^{-3} \text{ m}$  (Fig.5). It characterizes that the

smaller the diameter (i.e., smaller permeability and porous-radius equivalent, see Table III) of particle weakens the penetration. In  $d=10^{-3}$  m case, Fig.7 depicts channels occurrence for  $T_h/T_a=318/318$  K in the glass beads, but not in the alumina balls (Fig.6). It indicates that migration into the glass beads is faster. Thus, these evidences prove that the condensate migration does not depend only on permeability [3]-[5], surface tension [6], gravity [7], and porous-radius equivalent, but also influenced by wetting mechanism.

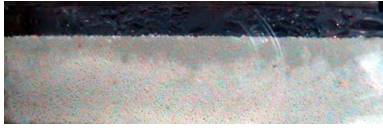


Fig.4 Alumina balls,  $T_h/T_a=328/328$  K in  $d=0.5 \times 10^{-3}$  m



Fig.5 Alumina balls,  $T_h/T_a=328/328$  K in  $d=10^{-3}$  m



Fig.6  $T_h/T_a=318/318$  K,  $d=10^{-3}$  m in Alumina balls



Fig.7  $T_h/T_a=318/318$  K,  $d=10^{-3}$  m in Glass beads.

With positive work of immersion, alumina balls are able to more spontaneously immerse to condensate, in the other words, the condensate can flow over the balls bed without any concentration gradient. On the glass beads, however, with negative work of immersion, the concentration gradient is needed to make precursor penetration. Otherwise, with higher work of adhesion, the condensate migrates stickier into alumina balls than that glass beads since bonding-energy between the condensate with the alumina balls is also higher. The bonding can be explained by hydrophilic character belongs to alumina balls caused by its wetting angle  $\theta$  is less than  $90^\circ$ . Conversely, smaller work of spreading on glass beads, i.e., lower bonding due to hydrophobic ( $\theta > 90^\circ$ ), yields the condensate can spread easier on the glass beads surface.

Refers to the wetting phenomena, it can be reconstructed that the condensate can immediately migrate down into the alumina balls bed but, with slower velocity. Whereas, faster velocity in the glass beads can happen but, need for a while, a higher condensate concentration gradient. These flow characters, in both glass beads and alumina balls, are in a good

agreement with experiment on water flux through hydrophobic and hydrophilic porous glass [21].

The phenomena also imply that the migration flow is depended on the porous bed properties, where in this case, meaning porous-bed hydraulic resistivity. These elucidate that the resistivity is not only influenced by porous radius equivalent, porosity, and permeability, but also controlled by wettability.

### C2. Effect of ambient temperature

For the same mixture temperature  $T_h$  but, different ambient temperature  $T_a$ , treatment 328/308 K is able to generate, i.e., sensitive, a channel in  $d=0.5 \times 10^{-3}$  m alumina balls at minute 30 (Fig.8), but not for treatment 328/328 K although at minute 60 (Fig.4). The same situation, channel does not occur for 318/318 K in  $d=10^{-3}$  m alumina balls although at minute 60 (Fig.6), whereas clearly appear at minute 18 for 318/308 K (Fig.9).



Fig.8 Alumina balls at minute 30, for  $d=0.5 \times 10^{-3}$  m and 328/308 K,



Fig.9 Alumina balls at minute 18, for  $d=10^{-3}$  m and 318/308 K.

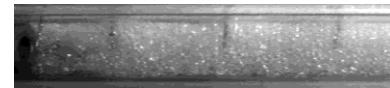


Fig.10 Top view of ceiling of chamber for  $T_h/T_a=1$

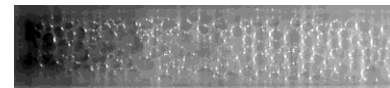


Fig.11 Top view of ceiling of chamber for  $T_a=308$  K.

It can be stated that the condensate migration dynamics increases, i.e., represented by channeling, with the lower  $T_a$ . In general, treatments  $T_a=308$  K can produce more channels than that  $T_h/T_a=1$ . This is not only caused by the more dropwise on the condensation-chamber's walls, depicted in Fig.11 (than that Fig.10), but also by the lower interface temperature  $T_s$  (Fig.2). The more dropwise on the walls is due to the more heat flux lost in  $T_a=308$  K treatments since  $T_a < T_h$ . Moreover, the lower  $T_s$  increases temperature difference between vapor dew-point  $T_d$  and  $T_s$ . This higher  $(T_d - T_s)$  raises a condensed vapor, i.e., filmwise condensate, on the interface.

The explanation reveals that the lower ambient temperature can produce more dropwise- and filmwise-condensate. Hence,

these raise the condensate concentration gradient between the interface and the porous bed, as a result, driven also by gravity [7], this gradient generates faster penetration or channel.

*D. Quantification of Migration Dynamics*

Practical Lyapunov Exponent  $L$ , using two attractors of nearest neighbors, has been proposed for quantifying dynamics in discrete cases [11],

$$L = \sum \log_2 (D_{n+1}/D_n) / N \quad (9)$$

However, it is necessary to note that, in each iteration, the value of the iterates, i.e.,  $D_{n+1}$  or  $D_n$ , must be substituted by a given initial constant separation  $D_0$ , (i.e.,  $D_0=10^{-6}$ ), to make  $D_{n+1}=D_n$ . Thus, the  $L$  is depended on the given constant.

In this study, to obtain the dynamics information, we use growth of distance  $S$ , between a point on the longest finger-front (as a lead-attractor) and on the nearest valley (as a lag-attractor) of the migrated condensate, as shown in Fig.12.

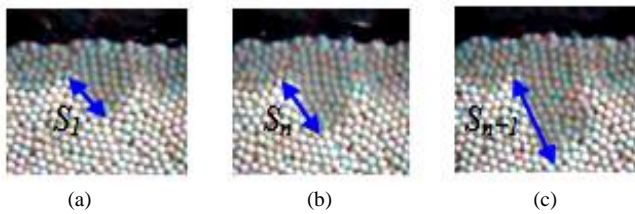


Fig.12 Propagation of the longest finger-front towards the nearest valley, from (a) to (c).

Due to the finger will never flow back, hence, if the given initial constant distance  $D_0$  is applied, then after the  $D_0$  is elapsed, the exponent series will be always in positive values although the leading attractor in stagnant toward the lagging one. It means no information, respectively, for retardation (stagnation), simultaneity, and convergence (lag-point moves to overtake lead-point) on the flow. Therefore, in this study, we also use an instantaneous Lyapunov-exponent series  $R_n$  as,

$$R_n = \log_2 (S_{n+1}/S_n) \quad (10)$$

Positive  $R$  means the finger propagates faster than the valley, otherwise, negative  $R$  indicates on faster propagation of the valley. Zero  $R$  can attribute to retardation, or simultaneous movement of the two points. By using a real distance growth and a determined period, the kinds of  $R$  can then distinguish between periodicity and nonperiodicity of the migration.

*E. Classification of Migration Dynamics*

Fig.13 and 14 depict respectively samples of dynamics of condensate distribution in  $d=0.5 \times 10^{-3}$  m and  $d=10^{-3}$  m alumina balls at  $T_h/T_a=318/318$  K treatment. Whereas, Fig.15 and 16 represent the distribution in  $d=10^{-3}$  m alumina balls and glass beads, respectively, for 328/328 K treatment.

Clearly, the dynamics distribution has a direct relation with the extracted condensate capacity. Afterwards, logically, the dynamics distribution is depended on the dynamics of

migration or penetration flow of the condensate through the media. Therefore, it is important to classify the migration dynamics to obtain their characters regarding extracted capacity prediction or any other implementations.

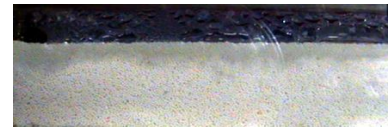


Fig.13 Alumina balls, 318/318 K in  $d=0.5 \times 10^{-3}$  m

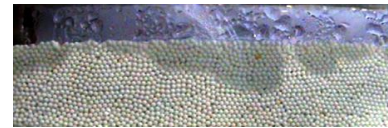


Fig.14 Alumina balls, 318/318 K in  $d=10^{-3}$  m

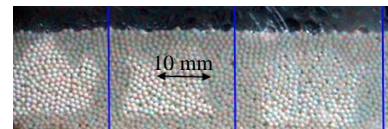


Fig.15 Channels in Alumina balls in  $d=10^{-3}$  m for 328/328 K.



Fig.16 Channels in Glass beads in  $d=10^{-3}$  m for 328/328 K.

Fig.17 snapshots migration history or dynamic series for the longest finger propagation on porous bed of alumina balls (AB), diameter  $d=0.5 \times 10^{-3}$  m, and treatment  $T_h/T_a=313/308$  K. And then, based on the  $R$  definition and the 3 minutes period, Fig.18 shows the  $R$  series of the snapshot.



N=1~7



N=8



N=9



N=10

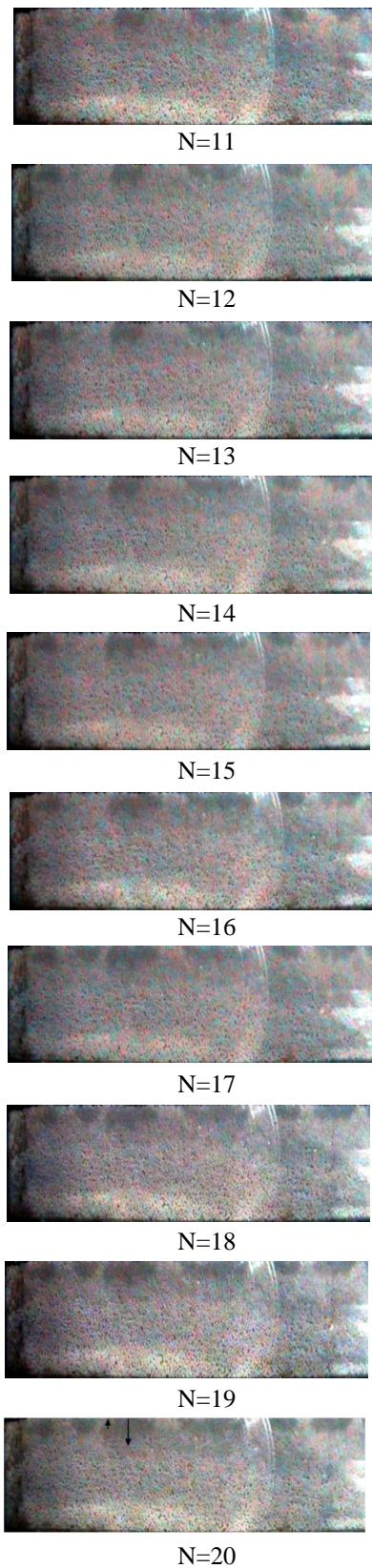


Fig.17 Snapshot of the longest finger propagation on alumina balls bed,  $d=0.5 \times 10^{-3}$  m,  $T_h/T_a=313/308$  K

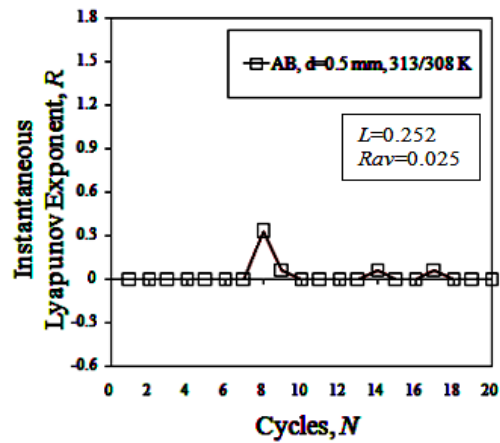


Fig.18  $R$  series based on snapshot of the longest finger propagation on AB,  $d=0.5 \times 10^{-3}$  m,  $T_h/T_a=313/308$  K

From the  $R$  series, on the Fig.18, the average instantaneous Lyapunov exponent  $R_{av}$  can then be calculated. Moreover, the Lyapunov exponent  $L$  based on the observed initial distance separation is obtained as well.

Subsequently, Fig.19 highlights propagation history or dynamic series on  $d=0.5 \times 10^{-3}$  m alumina balls for  $T_h/T_a=1$ , i.e., 308/308, 313/313, 318/318, 323/323, and 328/328 K, whereas Fig.20 is for  $T_a=308$  K treatments. The series show points of  $R=0$  dominate than that  $R \neq 0$ . As supported by Fig.4 and 13, some of the  $R=0$  attributes to retardation, due to have only thinner penetration. However, this migration is not strictly static, since Lyapunov exponent  $L$  is not zero (see Table IV). For this static-like penetration in the same period, we classify it as periodic-dominant or considerably uniform-flow migration. Leaning to uniform flow, this migration has least sensitivity, i.e., effectively insensitive, to generate a channel. For the channeling, a different behavior is found in 328/308 K, where channel occurs in this condition, shown in Fig.8. Thus, it is grouped on sensitive in channeling (see Table IV).

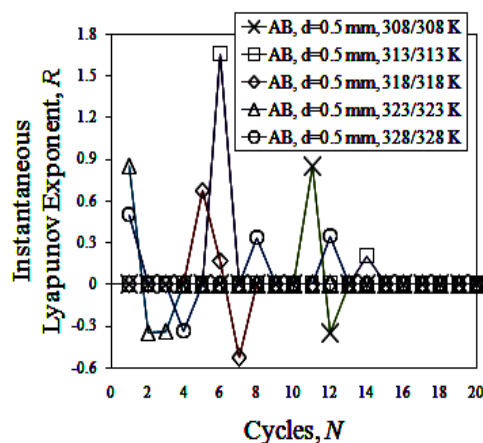


Fig.19  $R_n$  in alumina balls (AB),  $d=0.5 \times 10^{-3}$  m,  $T_h/T_a=1$

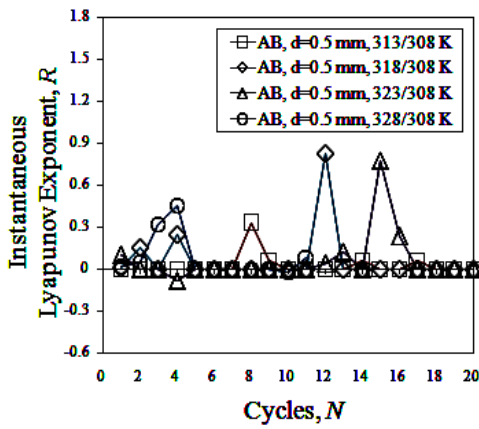


Fig.20  $R_n$  in alumina balls (AB),  $d=0.5 \times 10^{-3}$  m,  $T_a=308$  K

Unlike  $d=0.5 \times 10^{-3}$  m case, Fig.21 shows more ‘balance’ between number of  $R=0$  and  $R \neq 0$  points, at  $d=10^{-3}$  m alumina balls. It is easy to range these  $T_h/T_a=1$  treatments into the periodic-dominant subregime (see Table IV) since some of  $R=0$  represent simultaneous (periodic) propagation of both front and its valley. As shown in Fig. 5, this subregime has sensitivity to create a channel, and also finger (Fig.14), despite they are in the same periodic-dominant with the  $d=0.5 \times 10^{-3}$  m case (see Table IV). Contrarily, all series on Fig.22 or  $T_a=308$  K show the dominant of  $R \neq 0$ . Due to lot of  $R \neq 0$  points are in different values, then, we cluster it in nonperiodic-dominant subregime. In this subregime, furthermore, it is also found the pure of nonperiodicity of the  $R$  points. These fully-nonrepeated- and nonzero-points (black marked), then, we categorize it as a (temporal) chaotic propagation.

In the  $d=10^{-3}$  m and  $T_h/T_a=1$ , the most dynamics or fewer  $R=0$ , is found in glass beads, as shown in Fig. 23. This glass beads, e.g., in Fig.7 or 16, if compared to alumina balls, e.g., Fig. 5 or 15, may be less sensitive (but not insensitive) in ability to create more than one channel as that alumina balls. However, one chaotic case is found in this glass beads’ subregime, i.e., in 328/328 K (see Table IV), whereas not in those alumina balls.

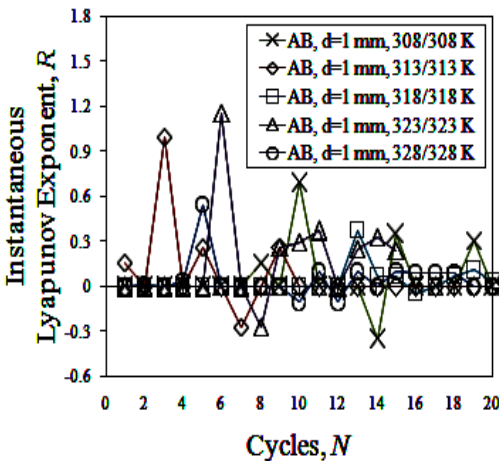


Fig.21  $R_n$  in alumina balls (AB),  $d=10^{-3}$  m,  $T_h/T_a=1$

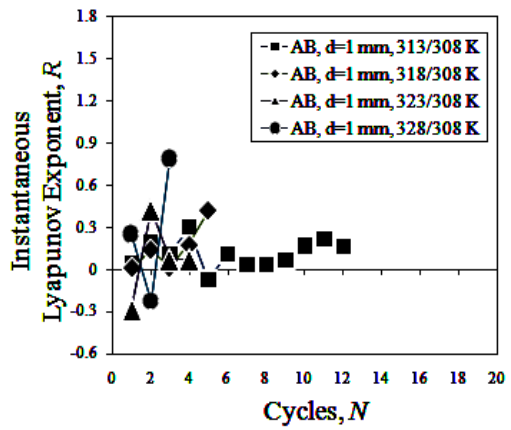


Fig.22  $R_n$  in alumina balls (AB),  $d=10^{-3}$  m,  $T_a=308$  K.

For  $T_a=308$  K and  $d=10^{-3}$  m, both in glass beads (Fig.24) and alumina balls (Fig.22) depict chaotic in all of  $T_h$  conditions. However, most of  $R$  points in glass beads are positive. It means finger propagation in glass beads is little bit more progressive.

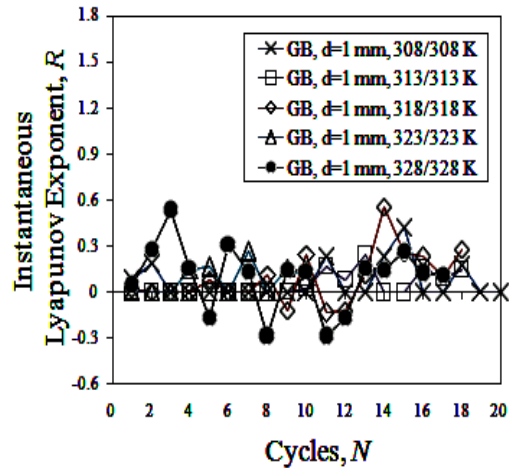


Fig.23  $R_n$  in glass beads (GB),  $d=10^{-3}$  m,  $T_h/T_a=1$

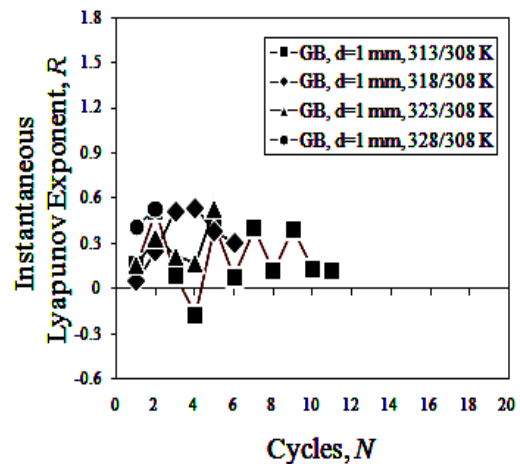


Fig.24  $R_n$  in glass beads (GB),  $d=10^{-3}$  m,  $T_a=308$  K.

In general, the  $T_a=308$  K treatments shorten cycles  $N$ , as displayed in Fig.21, 22, 23 and 24, except for  $d=0.5 \times 10^{-3}$  m (Fig.19 and 20). These reveal that  $T_a=308$  K and  $d=10^{-3}$  m accelerate finger propagation. It means that both alumina balls and glass beads having  $d=10^{-3}$  m are effective in extracting the moist. These are caused by higher in their porous radius equivalent  $r_{eq}$  and permeability  $K$  (see Table III). Furthermore, according to the wettability (i.e., the  $d=10^{-3}$  m alumina balls have higher both work of adhesion and immersion) and to the channel occurrence (i.e., in the same treatments, the alumina balls suppress two channels (Fig.15), but only one (Fig.16) for glass beads), it can then be concluded that, for the both  $d=10^{-3}$  m particles, the most effective in the extraction is alumina balls media.

TABLE IV  
SUB REGIME OF MIGRATION DYNAMICS

Particle [ $d \times 10^{-3}$ ]	$T_f/T_a$	$L$	$R_{av}$	Channel	Sub regime	case
Alumina Balls [0.5]	308/308	0.243	0.043			
	313/313	1.224	0.093			
	318/318	0.286	0.016			
	323/323	0.204	0.008	non		
	328/328	0.547	0.025	sensitive		
	313/308	0.252	0.025			
	318/308	0.673	0.062			
	323/308	0.316	0.058		periodic dominant	
Alumina Balls [1]	308/308	0.439	0.058			
	313/313	0.109	0.036			
	318/318	1.177	0.072			
	323/323	0.936	0.178			
	328/328	0.514	0.049			
	313/308	0.642	0.122			
	318/308	0.132	0.152			chaotic
	323/308	0.017	0.069			
Glass Beads [1]	328/308	0.093	0.272	sensitive		
	308/308	0.544	0.067			
	313/313	0.237	0.051			
	318/318	0.411	0.092		non periodic dominant	
	323/323	0.268	0.084			
	328/328	0.984	0.098			
	313/308	1.222	0.204			chaotic
	318/308	0.713	0.341			
323/308	0.455	0.286				
328/308	0.209	0.475				

For the migration regime, it is clearly that although the penetration flow is in (theoretical) Darcian regime, but this experimental study proves that the observed flow is not only considerably uniform (or periodic dominant), i.e., as expected in the regime, but also found nonuniform, even chaotic propagation in the some cases. In the chaotic propagation, corresponded to [2], this wetting process indeed unpredictable. Additionally, interesting phenomena, the unpredictable on the

wetting in a porous media is in fact similar with its drying process, or releasing moist. The study reported that it is impossible to predict drying rate on the porous solid with the help of heat and mass transfer theories, the drying rates must be obtained experimentally [22].

For the dynamics indicating, positive  $R_{av}$  compromises positive  $L$  (see Table IV), it means that the dynamics attributed by Lyapunov exponent  $L$  in [11] can also be indicated by the  $R_{av}$ . Moreover, the  $R_n$ , as the  $R_{av}$  component, can evaluate directly and give more dynamics information in each cycle. Therefore, it render that the  $R_n$  is not only suitable for indicating in long term, as the  $L$  can do, but also in short term or practical dynamics applications.

#### IV. CONCLUSION

Notably, the most effective treatments in generating channel, i.e., also finger, is  $T_a=308$  K on  $d=10^{-3}$  m alumina balls. Sequentially, ambient treatments have significant effect on the source of migrated condensate, i.e., condensate concentration gradient, on the interface. Afterward, in the propagation, it is not only porosity and permeability, but wettability components of media also control the hydraulic resistivity. Though the condensate migrates theoretically in Darcian regime, however, this experiment finds both stable (uniform) dominant and unstable (nonuniform) dominant on their propagation flow, even temporal chaos in some finger propagations.

Finally, for the modified practical Lyapunov exponent, due to simpler and able to inform more dynamics, it can be then proposed as indicator concept in practical or, especially in, short term dynamics applications.

#### ACKNOWLEDGMENT

We wish to thank Mr. Ryuichi Nagata, Mr. Maizul Majeed, and special for Mr. Takahiro Taguma for their valuable help in the experiments.

#### REFERENCES

- [1] D. P. Margaritis, Z. G. Diamantis, D. I. Poteinos, and D. T. Tsahalis, "Experimental and theoretical investigation of a capillary pumped loop," Proc. IASME/WSEAS int. conf. Energy and Environmental Syst., pp. 95-102, 2006.
- [2] L. L. Popovich, D. L. Feke, and I. Manas-Zlocover, "Influence of physical and interfacial characteristics on the wetting and spreading of fluid on powders," Powder Technology, vol. 104, pp. 68-74, 1999.
- [3] S. C. Wang, Y. T. Yang, and C. K. Chen, "Effect of uniform suction on laminar filmwise condensation on a finite-size horizontal flat surface in a porous medium," Int. J. of Heat and Mass Transfer, vol. 46, pp. 4003-4011, 2003.
- [4] S. C. Wang, C. K. Chen, and Y. T. Yang, "Film condensation on a finite size horizontal wavy plate bounded by a homogeneous layer," Applied Thermal Engineering, vol. 25, pp. 577-590, 2005.
- [5] S. C. Wang, C. K. Chen, and Y. T. Yang, "Steady filmwise condensation with suction on a finite-size horizontal flat plate embedded in a porous medium based on Brinkman and Darcy models," International Journal of Thermal Sciences, vol. 45, pp. 367-377, 2006.
- [6] T. B. Cang, and W. Y. Yeh, "Effects of uniform suction and surface tension on laminar filmwise condensation on a horizontal elliptical tube

- in a porous medium,” *International Journal of Thermal Sciences*, vol. 48, pp. 2323-2330, 2009.
- [7] R. Balasubramaniam, V. Nayagam, M. M. Hasan, and L. Khan, “Analysis of heat and mass transfer during condensation over a porous substrate,” *Ann. N.Y. Acad. Sci.*, vol. 1077, pp. 459-470, 2006.
- [8] Y. Katoh, S. Yamaguchi, and J. Kurima, “A study on condensation phenomena on a horizontal cooled flat plate in a porous medium,” *Transl. Japan, The JSME*, vol. 45, pp. 241-242, 2007.
- [9] E. Siswanto, Y. Katoh, and H. Katsurayama, “Condensation on the cooled plate surface under porous media controlled by the ambient temperature,” *Proc. 48<sup>th</sup> JSME Chugoku-Shikoku branch conf.*, Japan, pp.329-330, 2010.
- [10] E. Siswanto, Y. Katoh, and H. Katsurayama, “Forced laminar convective condensation in porous media”, *Proc. 47<sup>th</sup> National Heat Transfer Symp.*, Japan, pp. 135-136, 2010.
- [11] J. C. Sprott, “Automatic generation of strange attractors,” *Chaos & Graphics*, vol. 17, No. 3, pp. 325-332, 1993.
- [12] F. E. Udawadia, and H. F. von Bremen, “Computation of Lyapunov characteristic exponents for continuous dynamical systems,” *Z. Angew. Math. Phys.*, vol. 53, pp. 123-146, 2001.
- [13] Y. U. An, Z. Chen, C. Z. Sun, Z. Liu, K. Yan, and K. Warbinek, “Control of chaotic behavior in thruster motor system for deep water ocean robot,” *Proc. 6<sup>th</sup> WSEAS int. conf. Robotic, Control and Manufac. Technology*, pp. 68-71, 2006.
- [14] M. Stork, J. Hrusak, and D. Mayer, “Discrete-time chaotic systems impulsive synchronization and data transmission,” *Proc. 13<sup>th</sup> WSEAS int. conf. System*, pp. 127-132.
- [15] J. C. Sprott, J. C. Wildenberg, and Y. Azizi, “A simple spatiotemporal chaotic Lotka-Volterra model,” *Chaos, Soliton & Fractals*, vol. 26, pp. 1035-1043, 2005.
- [16] A. Singh, S. Lanzoni, and E. F-Georgiou, “Nonlinearity and complexity in gravel bed dynamics,” *Stoch. Environ. Res. Risk. Assess.*, DOI 10.1007/s00477-008-0269-8, Springer-verlag, 2008.
- [17] E. Zaman, and P. Jalali, “On hydraulic permeability of random packs of monodisperse spheres: Direct Flow Simulations versus Correlations,” *Physica A*, vol. 389, pp. 205-214, 2010.
- [18] A. R. Bogomolov, P. T. Petrik, and S. S. Azhikanov, “A study of heat transfer during steam condensation on a horizontal tube placed in granular material made of particles with different wettability of surface,” *Thermal Engineering*, vol. 56, No. 7, pp. 560-565, 2009.
- [19] Y. M. Chen and F. Mayinger, “Measurement of heat transfer at the phase interface of condensing bubble,” *Int. J. Multiphase Flow*, vol. 18, no. 6, pp. 877-890, 1992.
- [20] M. Kaviany, “Boundary-layer treatment of film condensation in the presence of a solid matrix,” *Int. J. Heat Mass Transfer*, vol. 29, No. 6, pp. 951-954, 1986.
- [21] G. T. Vladisavljevic, M. Shimizu, and T. Nakashima, “Permeability of hydrophilic and hydrophobic Shirasu-porous-glass (SPG) membranes to pure liquids and its microstructure,” *Journal of Membrane Science*, vol. 250, pp. 69-77, 2005.
- [22] F. Z. Angiz, N. Amanifard, and A. K. Haghi, “A numerical study on thermal drying of moist porous solid,” *Proc. 5<sup>th</sup> IASME/WSEAS int. conf. Heat Transfer, Thermal Eng., and Environment*, pp. 104-108, 2007.

**Eko Siswanto** is a Dr. Eng. candidate on Graduate School of Science and Engineering, Mechanical Engineering Department, Yamaguchi University, Japan. He works as a lecturer at Mechanical Engineering Department, Brawijaya University, Indonesia. His current research interest is thermal and multiphase flow dynamics on condensation in porous media.

**Asst. Prof. Hiroshi Katsurayama** did his Dr. Eng. from The University of Tokyo, Japan. His major field of study is aerospace engineering, and his current research interest is on hypersonic flow, and high enthalpy flow. He became a member of American Institute of Aeronautics and Astronautics (AIAA).

**Prof. Yasuo Katoh** did his Dr. Eng. of Mechanical Engineering from Kyushu University, Japan. His major field of study is applied thermal engineering and multiphase flow technology, and his current research interest is heat and mass transfer with phase change. He became a member of Japan Society of Mechanical Engineers (JSME) and Japanese Society for Multiphase Flow (JSMF).